UNCLASSIFIED

SECURITY CLASSIFICATION OF THIS PAGE

AD-A254 785

(1)

REPORT DOCUMENTATION

DTIC ELECTE AUG 24 1992 S C D

Form Approved OMB No. 0704-0188

1a. REPORT SECURITY CLASSIFICATION Unclassified	
2a. SECURITY CLASSIFICATION AUTHORITY N/A	3. DISTRIBUTION/AVAILABILITY OF REPORT Unlimited.
2b. DECLASSIFICATION/DOWNGRADING SCHEDULE N/A	
4. PERFORMING ORGANIZATION REPORT NUMBER(S)	5. MONITORING ORGANIZATION REPORT NUMBER(S)
6a. NAME OF PERFORMING ORGANIZATION Cornell University	6b. OFFICE SYMBOL (If applicable) N/A
7a. NAME OF MONITORING ORGANIZATION Office of Naval Research	
6c. ADDRESS (City, State, and ZIP Code) Office of Sponsored Programs 123 Day Hall Ithaca, NY 14853	7b. ADDRESS (City, State, and ZIP Code) Resident Representative N62927 Administrative Contracting Officer 33 Third Avenue - Lower Level New York NY 10003-9998
8a. NAME OF FUNDING/SPONSORING ORGANIZATION Department of the Navy	8b. OFFICE SYMBOL (If applicable)
9. PROCUREMENT INSTRUMENT IDENTIFICATION NUMBER N00014-89-J-1311	
8c. ADDRESS (City, State, and ZIP Code) Office of the Chief of Naval Research 800 North Quincy Street, Code 1513:CMB Arlington, VA 22217-5000	10. SOURCE OF FUNDING NUMBERS PROGRAM ELEMENT NO. / PROJECT NO. / TASK NO. / WORK UNIT ACCESSION NO.

11. TITLE (Include Security Classification)
"Innvoative Optoelectronic Materials and Structures using OMVPE"

12. PERSONAL AUTHOR(S)
James R. Shealy

13a. TYPE OF REPORT	13b. TIME COVERED	14. DATE OF REPORT (Year, Month, Day)	15. PAGE COUNT
Final Technical Status	FROM 1/1/90 TO 12/31/90	91/03/19	7

16. SUPPLEMENTARY NOTATION

17. COSATI CODES			18. SUBJECT TERMS (Continue on reverse if necessary and identify by block number)
FIELD	GROUP	SUB-GROUP	Semiconductors, Optoelectronics, Crystal Growth

19. ABSTRACT (Continue on reverse if necessary and identify by block number)

An advanced OMVPE process is being developed for the deposition of III-V semiconductor materials and structures. There are important optoelectronic device structures which can not be realized by conventional means. These include AlGaAs semiconductor lasers with improved coherence using embedded diffraction gratings, and GaInP pseudomorphic structures on GaP substrates for short wavelength semiconductor lasers. The structure on GaP result in improved laser performance compared to the 650 nm AlGaInP devices previously developed in this program. The new OMVPE apparatus combines the multichamber reaction cell with deep UV photo-assisted growth and modulation flow epitaxial techniques. Using a combination of such processes, the growth temperature requirements for III-V alloys can be substantially reduced. Selective growth on a sub-micron scale will be attempted with in-situ interference holography. The materials and techniques developed in this research program will result in significant simplifications to the fabrication sequence required to realize complex integrated optoelectronic circuits.

20. DISTRIBUTION/AVAILABILITY OF ABSTRACT	21. ABSTRACT SECURITY CLASSIFICATION
☒ UNCLASSIFIED/UNLIMITED ☐ SAME AS RPT. ☐ DTIC USERS	N/A
22a. NAME OF RESPONSIBLE INDIVIDUAL James R. Shealy	22b. TELEPHONE (Include Area Code) (607) 255-4057 / 22c. OFFICE SYMBOL

DD Form 1473, JUN 86 — Previous editions are obsolete. — SECURITY CLASSIFICATION OF THIS PAGE
UNCLASSIFIED

Table of Contents

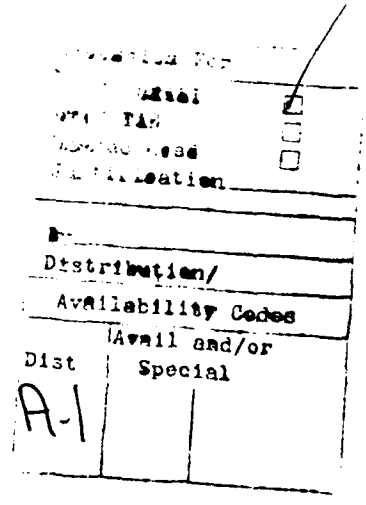

I. Introduction

Up until the end of 1990, this program has endured a transition period while the construction of Cornell's new OMVPE laboratory was completed. This lab offers a significant expansion of the OMVPE research facilitated by a conventional horizontal machine, the SDIO machine, and the multichamber apparatus recently donated by General Electric. In 1990, the research activities have focused on OEIC fabrication and materials characterization studies. The OMVPE reactor funded by this program will allow the first sub-micron selective growth studies, in-situ film characterization with a Raman probe, and advanced growth modes (ALE, FME, etc.) for advanced structures. This program will have profound impact on future OEIC development by combining the epitaxial deposition with microfabrication technologies.

The work unit consists of the principal investigator, 2 recently added Ph.D. candidates (Fall 1990) and one existing Ph.D candidate, all in the area of OMVPE growth. In addition, this program partially supports a research support specialist responsible for the OMVPE reactor construction. Finally, 1 Ph.D. supported by this program graduated in Aug. 1990 (S. O'Brien - OEIC Fabrication) while another student will graduate in May 1991 (T. Bradshaw - Raman Characterization).

II. Progress in the Past Year

The progress in the last year of this program has been highlighted below and appears in 4 sections. The first 2 sections are meant to give a brief update on the new facilities which supports compound semiconductor research activities at Cornell. Finally, key research activities which focus on quantum well laser materials and the fabrication of new OEICs will be discussed.

Langmuir Compound Semiconductor Materials Laboratory (LCSM)

In the year 1990, a concentrated effort was made to complete the LCSM facility and the introduction of 2 OMVPE reactors to the facility. The facility will be operational with a multichamber AlGaAs(GaInAs) reactor in early 1991. The exhaust treatment to remove the affluent from the gas stream which enters the environment was subject to an investigation by N.Y. State's Department of Environmental Conservation. Currently, State law requires a DEC permit for the use of the hydrides needed for OMVPE. Although this agency was most cooperative, this process resulted in lengthy delay in ordering and subsequent installation of the incineration/wet scrubbing system. Currently, as of March 1991, this is the only apparatus left to be installed to allow the operation of the first reactor. The facility's alarm system has been completed and is currently operational in a manual mode. When fully automated, the lab will have a "around the clock" computer "watch dog" capable of dialing out over the phone diagnostic messages via a speech synthesizer. Literally hundreds of parameters are continually monitored to insure proper operation and maintenance of the lab and its safety equipment. It is believed that US industry will find significant interest in this approach to provide a safe environment for OMVPE technology when it reaches major production status.

Reactor Design & Construction

The design of the SDIO reactor was essentially completed by the end of 1989. However, several iterations have been made during the construction, primarily in the cell design. Due to the inability of quartz manufacturers to build precision quartz bearings (required in the original design) for smooth, repeatable substrate rotation a design change was needed. Recall that this reactor is integrated into an optical bench to allow focused laser radiation to stimulate the growth. The mechanical design of the susceptor will probably limit the spatial resolution of the selectively growth features. For this reason, we have opted for a precision stainless steel bearing system. Early in this program, it was found that hot stainless steel will cause severe n-type contamination of the grown layers. Hence, the solution is the development of a cryogenic turn table for the susceptor support. This design change has had a major impact on the cell construction. It is anticipated that this reactor could commence operation in mid to late 1991. The gas handling system and the excimer pumped dye laser system has been completed and installed leaving only the reaction cell itself to be completed.

Optoelectronic Device Fabrication

The use of selective heterostructure disordering has profound impact on the fabrication of Optoelectronic Integrated Circuits (OEICs). The ability to intermix quantum well heterostructures opens the possibility to the fabrication and integration of novel optical devices since it allows the laterally controlled post growth alteration of the effective bandgap. By the end of 1989, our investigations included several III-V semiconductor structures. These include GaAs/AlGaAs on GaAs, GaInAs/AlGaAs on GaAs (pseudomorphic structures), GaInAs/AlInAs on InP and GaInP/AlInP on GaAs. The mechanism for the selective intermixing process was found to be either by an impurity free process (Ga vacancy diffusion) of by Si diffusion into the semiconductor from the SiO_2 film used to activate the process, depending on the III-V materials system. In 1990, we sucessfully fabricated OEICs on a single monolithic GaAs substrate using a combination of selective intermixing and other advanced fabrication processes available through the National Nanofabrication Facility at Cornell. Most noteworthy of these is the Chemically Assisted Ion Beam Etching (CAIBE) process for the fabrication of semiconductor laser facets and waveguide ridges. The OEICs fabricated and tested include multiple wavelength laser arrays, laser/external modulators, surface emitting ring cavity lasers (in collaboration with SRI-Sarnoff), and laser/internal cavity modulators.

Results on each of these monolithic circuits are given in Steve O'Brien's Ph.D. thesis attached to this report. A second integration of the ring laser device is currently underway. The laser/internal cavity modulator and its test results will be briefly discussed below to give a representation of the on going device research in this program.

The fabrication of an OEIC which features a laser and an intracavity modulator demonstrates the ability for the impurity free intermixing process to alter the semiconductor structures bandgap within a pin structure. This has been accomplished without significant alteration of the diodes IV characteristic. Reverse biases on the modulator section as large as 9 volts can be sustained with little leakage. This was accomplished

because of the adequate electrical isolation (typically 1.5 kΩ) between the laser gain section and intracavity modulator obtained with the CAIBE etched separation region. The basic operating principle is the quantum confined Stark effect in the reversed bias modulator section. Under no bias, the modulator absorption edge was shifted solely by the intermixing process such that it became transparent to the laser on the same host epitaxy. Application of reverse modulator bias introduces loss in the laser cavity resulting in a modulation depth of 25 dB at -5 volts. OEICs of this type could serve as replacements of laser/transistor driver OEIC designs as both offer a high impedance input and roughly the same high speed performance.

Materials Characterization

In 1990, work has focussed on characterization by Raman spectroscopy of $(InAs)_m/(GaAs)_m$, $(InAs)_m/(AlAs)_m$ and $(Al_{.3}Ga_{.7}As)_m(In_{.3}Ga_{.7}As)_m$ superlattices grown by MBE or Migration Enhanced Epitaxy. The values of m for our samples are between two and eight. Besides their potential device applications, these short period strained layer structures are interesting from a fundamental viewpoint. Phonons and electrons in layered media display the effects of zone folding and quantum confinement which are, in turn, sensitive indicators of material structure and quality. The $(InAs)_m/(GaAs)_m$ and $(InAs)_m/(AlAs)_m$ layers were grown on $Al_{.48}In_{.52}As$ buffer layers lattice matched to InP substrates; consequently, the GaAs or AlAs (InAs) layers are expected to be under tensile (compressive) strain due to the relatively large lattice mismatch (3.8%). In addition to the usual quantum confinement effects, LO phonons in these materials should exhibit energy shifts on the order of several wavenumbers due to strain. Because the energies of the zone center GaAs–like modes in $Al_{.3}Ga_{.7}As$ and $In_{.3}Ga_{.7}As$ are nearly equal, the possibility for propagative optical modes in $(Al_{.3}Ga_{.7}As)_m(In_{.3}Ga_{.7}As)_m$ superlattices exists.

Various lines of the Ar^+ laser were used to record the Raman spectra of these samples. In the backscattering geometry used, phonons belonging to the irreducible representations A_1 and B_2 of the symmetry group D_{2d} of the superlattice are observed in the polarized or depolarized spectra, respectively. The measured energies of the zone folded acoustic modes are in good agreement with calculations based on the elastic continuum (Rytov) model. Two orders of folded modes were observed in the 4 and 8 monolayer (InAs)/(GaAs) and $Al_{.3}Ga_{.7}As)/(In_{.3}Ga_{.7}As)$ samples. For the $(InAs)_4/(GaAs)_4$ layer, comparison of the measured intensities with predictions based on the photoelastic effect indicates some deviation from perfectly abrupt interfaces.

With the exception of the $(InAs)_8/(GaAs)_8$ sample, which displayed poor RHEED characteristics, LO phonons in these layers show clear evidence of strain shifts and quantum confinement. Three orders of confined GaAs phonons were observed in the $(InAs)_4/(GaAs)_4$ sample. To confirm the existence of a propagative LO mode in the $(Al_{.3}Ga_{.7}As)_m(In_{.3}Ga_{.7}As)_m$ structures, these samples were Si doped at 10^{18} cm^{-3}. A propagative LO phonon coupled to the plasmon was observed at an energy consistent with the doping level and independent of the superlattice period. Use of longer wavelength excitation (550–650 nm) allowed depth profiling through the entire epilayer. These measurements indicated that uniform strain exists in these layers.

The Raman characterization of semiconductor lasers was continued in 1990. Several structures were examined and the non-resonant spectra of single quantum well GRIN-SCH structures were reported at the end of 1989. A continued investigation of other laser designs including MQW structures from Spectra Diode Labs and OMVPE and MBE grown AlGaAs DH and SCH structures. In most all cases the active region of these devices yielded measurable Raman features giving information on the structure in the waveguide core. However, in some cases photoluminescence presumed to be from the degenerately doped GaAs cap layer interfered with the Raman (typically near 930 nm). It was of considerable interest to study to phonon dynamics of laser operation by examining Raman spectra under forward bias. In all samples, attempts to observe the Raman features of these lasers under operation failed due to interfering electroluminescence (or photoluminescence stimulated by the laser emission). Even lasers whose wavelengths were as short as 750 nm suffered from IR emission of sufficient strength to swamp the Raman scattered light. Special structures could possibly be grown to avoid these problems (i.e. thick cladding regions with AlGaAs capping regions).

III. Publications & Presentations

Publications

1. S. O'Brien, J.R. Shealy, D.P. Bour, L. Elbaum, and J.Y. Chi,"Effects of Rapid Thermal Annealing and SiO_2 Encapsulation on GaInAs/AlInAs Heterostructures," *Appl. Phys. Lett.*, **56** (April 1990), 1365-7.

2. J. Bradshaw and J.R. Shealy,"Characterization of GaAs/AlGaAs Graded Index-Separate Confinement Heterostructure Lasers by Raman Scattering," *J. Appl. Phys.*, **68** (July 1990), 358-360.

3. J. Bradshaw and J.R. Shealy,"Characterization of GaAs/AlGaAs Graded Index-Separate Confinement Heterostructure Lasers by Raman Scattering," *CLEO Technical Digest*, **7** (1990), 14-6.

4. A. Behfar-Rad, J. R. Shealy, S. R. Chinn, and S. S. Wong,"Effect of Cladding Layer Thickness on the Performance of GaAs/AlGaAs Graded Index Separate Confinement Heterostructure Single Quantum Well Lasers," *IEEE J. Quantum Elec.*, **26** (Feb. 1990), 1476-80.

5. S. O'Brien, J.R. Shealy, V.K.F. Chia, and J.Y. Chi ,"Selective Interdiffusion of GaInAs/AlInAs Quantum Wells by SiO_2 Encapsulation and Rapid Thermal Annealing," *J. Appl. Phys.*, **68** (November 1990), 5256-5261.

6. S. O'Brien, J.R. Shealy, and G.W. Wicks,"Monolithic Integration of an (Al)GaAs Laser and an Intracavity Electroabsorption Modulator using Selective Partial Interdiffusion," *Appl. Phys. Lett.*, **58** (April 1991).

Presentations

1. J. Bradshaw and J.R. Shealy,"Characterization of GaAs/AlGaAs Graded Index-Separate Confinement Heterostructure Lasers by Raman Scattering," *CLEO*, Anahiem, Ca. (May 1990).

2. J.R. Shealy,"Technology Requirements for OMVPE Growth of III-V Compounds," *Joint ARO/ETDL Workshop - Chemistry Related to Semiconductor Growth Involving Organometallics*, Fort Monmouth, N.J. (May 1990).

3. J.R. Shealy,"Modern Growth Techniques for Epitaxial III-V Semiconductors," *14th Nordic Semiconductor Meeting*, Denmark (June 1990).

4. S. O'Brien,"Wavelength Tunable Lasers using Selective Partial Intermixing," *IEEE Conference on Integrated Photonics Research (Topical meeting)*, Monterey, CA (April 9-11, 1991).

5. S. O'Brien, J.R. Shealy, and G.W. Wicks,"Monolithic Integration of an (Al)GaAs Laser and an Intracavity Electroabsorption Modulator using Selective Partial Interdiffusion," *CLEO/QELS*, Baltimore, MD (May 12-17, 1991).

IV. Summary

In the past, SDIO program has strengthened the III-V semiconductor materials related activities at Cornell and has presently provided support for optoelectronic devices related research. The first functional OEICs emerged from this program in the last year. Transistion of this program's technology to US industry and government labs has always been a priority. This transfer of technology has recently been facilitated by the transfer of people, S. O'Brien to Spectra Diode Labs and J. Singletery (only partially supported by this program) to JPL. Currently, Spectra Diode has obtained expertise in the selective impurity free intermixing process technology and JPL has benefited from the addition of an experienced OMVPE grower to their staff.

Characterization of GaAs/AlGaAs graded index-separate confinement heterostructure lasers by Raman scattering

J. Bradshaw and J. R. Shealy
School of Electrical Engineering, Cornell University, Ithaca, New York 14853

(Received 5 October 1989; accepted for publication 27 February 1990)

We report the first use of Raman scattering to study GaAs/AlGaAs graded index-separate confinement heterostructure quantum-well lasers. We have used a forward scattering geometry in which the waveguide is endfired, and the light emerging from the opposite end facet is collected and spectrally analyzed. The probe is confined by the waveguide and thus interacts with the entire laser cavity. Because Raman scattering occurs in all regions of the heterostructure to which the optical mode is confined, this technique is a useful indication of the mode profile in waveguide heterostructures. We observe inhomogeneously broadened longitudinal and transverse optical phonons in the graded region.

During the past decade the Raman effect has proved to be a valuable tool for studying elementary excitations in III-V materials and heterostructures as well as for characterizing such basic properties as band offsets, ternary composition and electron mobility.[1-3] In most of these studies the sample was excited with a visible laser in a backscattering geometry. This is adequate for the majority of characterization problems; however, nondestructive study of a single thin film located beneath several thousand angstroms of material is, at best, difficult because of the limited penetration depth of the probe and the small film thickness. Previous attempts[4] to study single quantum wells by Raman scattering required resonant excitation at liquid-He temperatures. In particular, the problem of thin film characterization arises in the study of laser heterostructures in which an active region a few hundred angstroms wide is located beneath typically a half micron cladding layer. The obvious solution in this case is to use the waveguide in order to confine the Raman probe beam to the region of interest in the device. In fact, this work is analogous to past experiments in optical fibers and dielectric waveguides[5-9] that demonstrated two unique properties of the waveguide as a medium for light scattering: one, thresholds for nonlinear processes are usually lower in the fiber because the energy density of the guided mode is normally greater than that of plane waves in the bulk, and two, because the intensity of the scattered light is

 0021-8979/90/130358-04$03.00

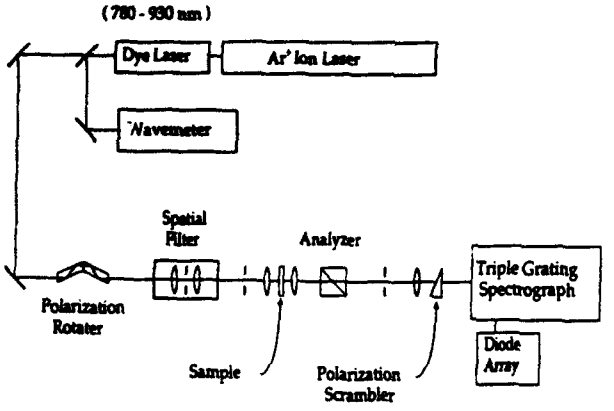

FIG. 1. Experimental apparatus.

proportional to the optical path length of the probe beam, the use of long fibers facilitates observation of weak signals. In their study of polymethacrylate thin films, Levy and Dupeyrat[9] estimated that incorporation of the film in a dielectric waveguide resulted in an increase in spontaneous Raman scattering by about three orders of magnitude. To our knowledge, this is the first study to obtain similar results with the III-V material system.

Figure 1 shows a diagram of the experimental apparatus. The output beam of an Ar^+-pumped Styryl 9 M *cw* dye laser (780–930 nm) was focused with a 0.50 NA (numerical aperture) microscope objective to an approximately 1.8-μm diam. spot on a (110) cleavage plane of the device. After passing through a broadband (700–1000 nm) polarization rotator, the incident beam was spatially filtered. A 0.6 NA objective was used to image the near-field radiation pattern on a slit which blocked any stray unguided light collected by the objective at the exit facet. This stray light was usually quite weak. The desired polarization of the scattered light was selected with a polarizing beamsplitter. Finally, the light passed through a focusing lens and polarization scrambler before entering a triple grating spectrograph. The scattered light was detected with a 1024 element diode array controlled by an optical multichannel analyzer. The power of the dye laser beam was approximately 10 mw at 905 nm. This wavelength was selected to be well below the fundamental absorption edge of the active region. All spectra were taken in the forward scattering geometry at 300 K.

Figure 2 shows spectra of the graded index-separate confinement heterostructure (GRIN-SCH) laser of Fig. 3 taken in two different polarization configurations. In the waveguide, the boundary conditions imply that light scattering occurs between laterally confined wave-packet states, unlike scattering between plane waves in bulk. It is apparent that the spectrum is strongly dependent on the polarization of the incident and scattered guided modes. When both modes are polarized parallel to a [110] crystal direction, both longitudinal and transverse phonons are seen, whereas if the incident and scattered modes are cross polarized, only vibrations at the transverse frequency appear. We observed no scattering when both modes are polarized along the [001] growth direction. GaAs-like and AlAs-like longitudinal optical (LO) vibrations and the GaAs-like transverse optical (TO) phonon of the graded index region are evident as well as the LO phonon of the quantum well. The latter is a shoulder on the high-energy side of the GaAs-like LO. The TO phonon in the quantum well cannot be resolved from the inhomogeneously broadened GaAs-like TO feature of the graded layer. Small displacements of the input dye laser beam at the end facet of the sample caused the relative strength of the quantum well and graded index features to vary, indicating the sensitivity of the spectrum to the incident guided mode. In this context, Raman spectroscopy is a

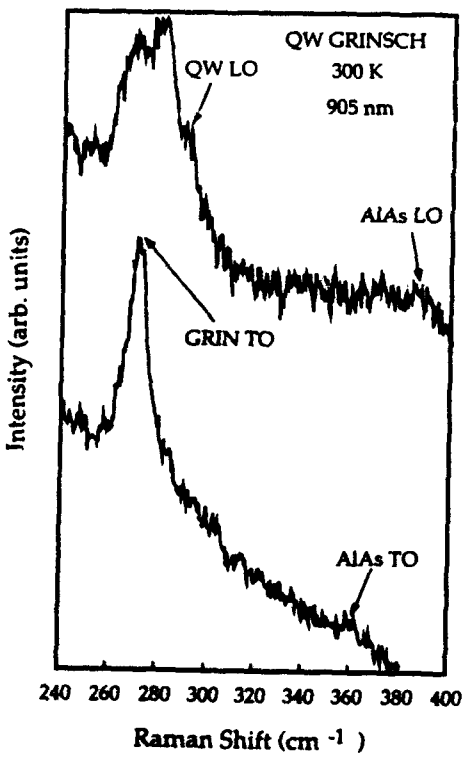

FIG. 2. In the top scan polarization of incident and scattered guided modes lies parallel to a [110] crystal direction. In the bottom scan the incident polarization is parallel to the [001] growth direction. First-order Stokes Raman spectra of the GRIN-SCH laser.

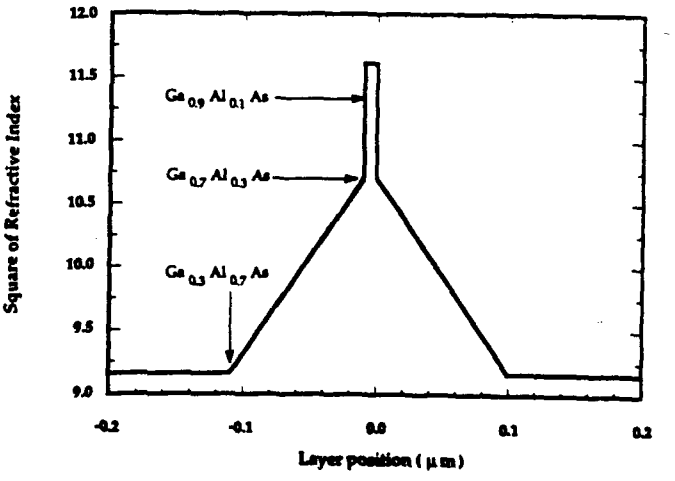

FIG. 3. GRIN-SCH laser structure used in this experiment.

useful indication of guided mode profile because the signal strength of a particular excitation is proportional to the intensity of the optical mode in the corresponding region of the heterostructure.

Significant effort has been directed at studying the vibrational properties of thin ionic slabs in III-V systems by Raman scattering.[10-12] These vibrational modes fall into two distinct categories: longitudinal and transverse vibrations confined to the slab by the material discontinuity and interface modes which are atomic displacements that damp exponentially away from the interface. Unlike most of these studies which use backscattering, conservation of momentum for the forward scattering geometry used in this work restricts observation to those vibrational modes whose wave vector is parallel to the direction of propagation of the optical probe and which thus lie in the plane of the slab. Zucker *et al.*,[10] in their study of the vibrational modes in a multiquantum-well sample consisting of 65 periods of 96-Å GaAs embedded between 98-Å $Al_{0.28}Ga_{0.72}As$ barriers, used a right-angle geometry in which the incident light propagated along the [001] growth direction, and the scattered light was collected normal to a [110] face. Because of the discontinuity in material, optical phonons cannot propagate normal to the layers. Thus in their experiment the phonon wavevector also lay along a [110] direction in the plane of the quantum well. They observed only longitudinal and transverse vibrations confined in the GaAs wells. Although our spectra are complicated by the prescence of features associated with the graded index layers, the polarization behavior of the quantum-well phonon is similar to the LO feature observed by Zucker.

Arora *et al.*,[11] in a Raman scattering study of interface modes in GaAs/AlGaAs superlattices, found that the intensity of these modes relative to the GaAs LO depends on the quality of the interface; less perfect interfaces show stronger interface mode scattering. The high performance of this particular laser material[12] (threshold current densities less than 250 A/cm^2) leads us to expect consistently excellent material characteristics of the quantum well, interface, and graded regions and hence that the GaAs LO would dominate the Raman spectrum. Because of the similar polarization dependence of the quantum-well feature seen in this work to that noted by Zucker and co-workers, and the data of Arora *et al.*, we believe the feature at 289 wave numbers to be a longitudinal vibration confined in the GaAs quantum well. The small shift from the bulk indicates alloying in the well on the order of 10%.

The GaAs-like LO and TO features of the graded index region occur at 279 and 269 wavenumbers, respectively. This corresponds to 30% AlGaAs,[2] the lower composition of the GRIN region where the optical mode is most intense. The full-width at half-maximum (FWHM) of the LO feature, however, is considerably broader than the linewidths previously reported[13,14] for this material because of the wide composition grading. Parayanthal and Pollak[13] have shown that the broadening and asymmetry of the LO phonon spectrum in bulk alloy semiconductors can be calculated using a spatial correlation model. Within that framework, the Raman intensity can be written as

$$I(\omega,L) \propto \int_0^1 \exp\left(\frac{-q^2L^2}{4}\right) \frac{d^3q}{[\omega-\omega(q)]^2+(\Gamma_0/2)^2}. \quad (1)$$

In Eq. (1), L, the spatial correlation length, is infinite for binary material. Γ_0 is the natural linewidth of the Raman transition for the binary, and q, the phonon wave vector, is in units of the Brillouin zone edge. Attempts to apply this to Raman scattering in a graded layer by calculating a superposition of such line shapes weighted by the mode intensity were unsuccessful. This is probably due to the difficulty in determining a suitable set of values of L, since the coherence length is not uniquely determined by the ternary composition, but depends on other factors as well.[13] Despite this, qualitative comparison of spectra taken from a variety of samples should reveal significant information, however. One would expect wider spectral lines from samples with broader grading limits, for example, and structures with wider quantum wells should give proportionately larger well to GRIN signal ratios.

The immediate applications of this work include characterization of single pseudomorphic thin films, which are currently of great interest for electronic and optical applications, and the study of fundamental processes in semiconductor lasers. Recently there has been some indication that photoexcited LO phonons may participate in stimulated emission in $GaAs/Al_xGa_{1-x}As$ quantum-well heterostructures.[15,16] Such nonequilibrium phonon distributions should be readily observable with Raman spectroscopy.[17] Study of electron-phonon coupling and the single-particle and collective excitations of the degenerate Fermi gas[18] of electrons and holes in a forward biased device could yield much information about many-body processes in semiconductor lasers.

We wish to thank Dr. S. R. Chinn of G. E. Electronics Laboratory for useful discussions. The support of SRI-David Sarnoff Research Center Contract No. C900154, the Joint Services Electronics Program Contract No. F49620-87-C-0044 and Innovative Science and Technology Contract No. N00014-89-J-1311 is also gratefully acknowledged.

[1] J. Menendez, A. Pinczuk, D. J. Werder, A. C. Gossard, and J. H. English, Phys. Rev. B 33, 8863 (1986).
[2] G. Abstreiter, E. Bauser, A. Fischer, and K. Ploog, Appl. Phys. 16, 345 (1978).
[3] R. Tsu, in *Proceedings of the Society of Photo-optical Engineers*, edited by D. E. Aspnes, S. So, and R. F. Potter (Society of Photo-optical Engineers, Bellingham, Washington, 1981), Vol. 276, p. 78.
[4] A. Arora, E. K. Suh, A. K. Ramdas, F. A. Chambers, and A. L. Moretti, Phys. Rev. B 36, 6142 (1987).
[5] R. H. Stolen, in *Proceedings of the Third International Conference on Light Scattering in Solids*, edited by M. Balkanski, R. C. C. Leite, and S. P. S. Porto (Flammarion, Paris, 1976), p. 656.
[6] R. H. Stolen, J. E. Bjorkholm, and A. Ashkin, Appl. Phys. Lett. 24, 308 (1974).
[7] E. P. Ippen, Appl. Phys. Lett. 16, 302 (1970).
[8] R. H. Stolen, Appl. Phys. Lett. 20, 63 (1972).
[9] Y. Levy and R. Dupeyrat, J. Phys. C 5, 38, 253 (1977).
[10] J. E. Zucker, A. Pinczuk, D. S. Chelma, A. Gossard, and W. Wiegmann, Phys. Rev. Lett. 53, 1280 (1984).
[11] A. Arora, A. K. Ramdas, M. R. Melloch, and N. Otsuka, Phys. Rev. B 36, 1021 (1987).
[12] J. R. Shealy, Appl. Phys. Lett. 52, 1455 (1988).

[13]P. Parayanthal and F. Pollak, Phys. Rev. Lett. 52, 1822 (1984).
[14]B. Jusserand and J. Sapriel, Phys. Rev. B 24, 7194 (1981).
[15]N. Holonyak, Jr., D. W. Nam, W. E. Plano, E. J. Vesely, and K. C. Hsieh, Appl. Phys. Lett. 54, 1022 (1989).
[16]H. H. Dai, M. S. Choi, M. A. Gunderson, H. C. Lee, P. D. Dapkus, and C. W. Myles, Appl. Phys. Lett. 66, 2538 (1989).
[17]J. Shah and J. C. V. Mattos, in *Proceedings of the Third International Conference on Light Scattering in Solids*, edited by M. Balkanski, R. C. C. Leite, and S. P. S. Porto (Flammarion, Paris, 1976), p. 145.
[18]A. Mooradian, in *Proceedings of the International Conference on Light Scattering Spectra of Solids*, edited by G. Wright (Springer, Berlin, 1969), p. 285.

Effects of rapid thermal annealing and SiO_2 encapsulation on GaInAs/AlInAs heterostructures

S. O'Brien and J. R. Shealy
School of Electrical Engineering, Phillips Hall, Cornell University, Ithaca, New York 14853

D. P. Bour and L. Elbaum
David Sarnoff Research Center, CN 5300, Princeton, New Jersey 08543-5300

J. Y. Chi
GTE Laboratories Inc., 40 Sylvan Road, Waltham, Massachusetts 02254

(Received 12 October 1989; accepted for publication 23 January 1990)

Substantial blue shifts in the transition energies of GaInAs/AlInAs single quantum wells were observed due to localized SiO_2 capping and rapid thermal annealing at temperatures between 750 and 900 °C. In contrast to previously reported results, regions capped with SiO_2 exhibited blue shifts up to 74 meV while regions with no SiO_2 showed minimal shifting. With this band-gap change, a lateral index change of approximately -0.6% is anticipated making this process suitable for index-guided lasers. Samples also exhibited up to 15-fold increases in PL efficiencies due to the annealing process. The dependence of energy shifts and PL efficiencies is studied by measuring room-temperature and low-temperature photoluminescence.

The ability to engineer the optical and electrical properties of semiconductor crystals by the precise epitaxial growth of special vertically layered structures has produced numerous state-of-the-art optical and electical devices.[1,2] However, the integration of optical and/or electrical devices (such as lasers, detectors, waveguides, and transistors) also requires lateral control over the electrical and optical properties. The partial intermixing of layered structures will significantly alter the material properties and can, for example, be used to selectively change the absorption properties yielding a variety of possible applications.[3,4] Methods such as impurity diffusion, impurity implantation, and laser irradiation have been used to intermix semiconductor heterostructures. In addition, SiO_2 encapsulation and rapid thermal annealing,[3] or furnace annealing,[5] has also been used to intermix GaAs/AlGaAs heterostructures. Presently, a majority of the optical applications coincide with optical fiber communication systems and require devices operating in the 1.3–1.55 μm range. In this work we have observed the blue shifting of GaInAs/AlInAs quantum well transitions (1.11–1.46 μm) by as much as 74 meV and is attributed to the intermixing of group III elements near the interfaces. With this band-gap change, a lateral index change of approximately -0.6% can be anticipated making this process suitable for index-guided lasers. The selective intermixing was accomplished by the deposition of SiO_2 followed by rapid thermal annealing (RTA) and contrary to previously published results,[6] the intermixing occurs under regions capped by SiO_2. These results conform to very similar experiments performed in other III-V semiconductor material systems.[3,7,8] The RTA process also dramatically improved the photoluminescence (PL) efficiencies for wells which were not significantly intermixed.

The samples were grown lattice matched on a sulfur-doped InP substrate by molecular beam epitaxy and consisted of a buffer layer which included a ten-period superlattice containing 13 Å InGaAs wells with 300 Å AlInAs barriers. The upper portion of the layer contained four single quantum wells ranging in nominal thickness from 20 to 66 Å separated by 300 Å barriers with the thinner wells closer to the surface. The growth finished with a 3000 Å AlInAs layer. All layers were nominally undoped. The PL linewidths at 5 K, as measured by the full width at half maximum, for the quantum wells varied between 10 and 20 meV while the linewidth of the AlInAs was 18 meV. A 3000 Å layer of electron beam evaporated SiO_2 was deposited on half of each sample and rapid thermally annealed at temperatures between 750 and 900 °C for 15 s in an argon ambient using pieces of undoped GaAs substrate for proximity caps.

Room-temperature and low-temperature ($\simeq$80 K) PL spectra were measured on all samples using the 5145 Å line of an argon-ion laser. Figure 1 shows the 80 K PL spectra from the SiO_2-capped regions of samples annealed at 850 and 900 °C along with the bare region of a sample annealed at 750 °C. The peak positions for the bare sample annealed at 750 °C and the as-grown material are identical. Significant blue shifting is clearly evident for the SiO_2-capped regions. No shifting was observed in the 80 K PL for the SiO_2-capped or bare regions of samples annealed at 700 and 750 °C. The observed 80 K PL shifts for the SiO_2-capped regions for the 850 and 900 °C anneals are shown as a function of well width in Fig. 2. The solid lines represent the shift of the SiO_2-capped region with respect to as-grown material while the dashed lines represent the shift of the SiO_2-capped region with respect to the bare region of the same sample. For the 850 °C anneal the dashed curve overlays the solid curve. Unlike the results of Chi *et al.*, where shifting occurred for the uncapped regions,[6] significant shifting occurs for the SiO_2-capped regions with very little shifting occurring for the bare regions. The results presented here are consistent with very similar experiments performed on GaAs/AlGaAs,[3] GaInP/AlInP,[7] and GaInAs/(Al)GaAs[8] quantum well structures. The effects of arsenic overpressure on the formation of defects which promote diffusion can be dramatic and can explain the results of Chi *et al.*[9] In the present work the samples were capped with undoped GaAs substrate material which

 0003-6951/90/141366-03$02.00

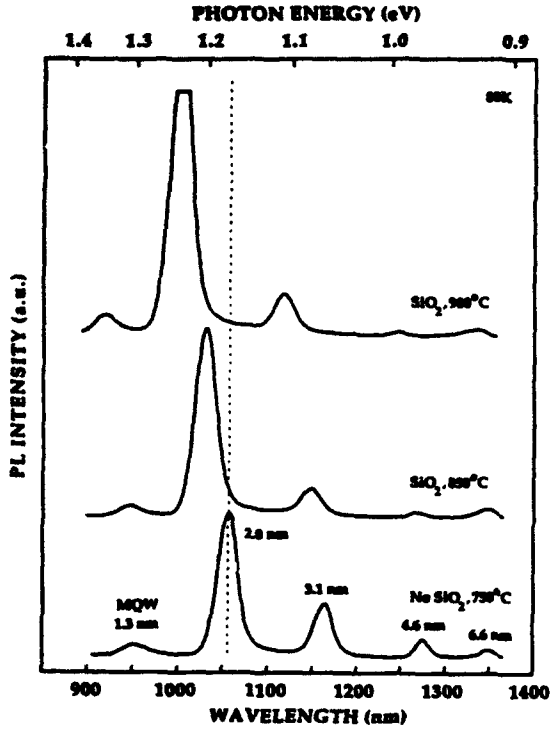

FIG. 1. 80 K PL spectra from the AlInAs/GaInAs samples containing a multiple quantum well buffer and four single quantum wells annealed at various temperatures with or without SiO_2 capping.

protects the surface from As or In desorption by providing an effective overpressure yet the samples of Chi *et al.* were not capped enabling significant As and In desorption creating, for example, column III vacancies and hence significant group III diffusion.[9] Blue shifting was observed by Miyazawa *et al.* for SiN_x-capped GaInAs/AlInAs wells which were repetitively rapid thermally annealed where one cycle RTA produced the same amount of shifting for both capped and uncapped regions.[10] The mechanism causing the intermixing under the SiO_2 is not known but could be due to a group III vacancy diffusion process[3] or a Si impurity-induced process.[11] A secondary-ion mass spectroscopy (SIMS) analysis of GaAs/AlGaAs superlattices which were intermixed using the same process showed no appreciable Si, yet Si incorporation into the GaInAs/AlInAs structures cannot be ignored by analogy since for intermixed GaInP/AlInP superlattices SIMS analyses showed additional Si ($\sim 10^{18}$ cm^{-3}).[7] The effects of strain at the dielectric-semiconductor interface could also be important for either diffusion mechanism. Room-temperature PL spectra (data not shown) consisted of two main peaks located at approximately 1.12 and 1.24 μm corresponding to the 20 and 31 Å wells, and a small peak at approximately 1.36 μm corresponding to the 46 Å well. The same shifting was clearly evident in the room-temperature PL with the only difference being that the relative shifting (w.r.t. as-grown material) was approximately a constant 14 and 6 meV higher for the 20 and 31 Å wells, respectively.

Intermixing can also strongly affect the PL efficiencies from the wells. Figure 3 shows the PL efficiencies, normalized to the as-grown sample, from the 31 Å well as a function of annealing temperature for the SiO_2-capped and bare regions. The bare regions show definite increases in PL efficiency, where for the 900 °C anneal the PL efficiency has increased 7-fold. The 66 Å well showed a 15-fold increase in PL efficiency. Similar results have been observed by Seo *et al.*[12] GaAs/AlGaAs structures similarly annealed do not exhibit this effect and is likely due to the inherent native defect types and densities for the two material systems. Intermixing is clearly evident by the sharp decrease in PL efficiency from the SiO_2-capped regions for those temperatures where blue shifting occurred. Such a decrease is consistent with the presence of Al in the well since AlInAs typically exhibits reduced PL efficiencies due to associated defects. It should be noted that PL efficiencies for the intermixed wells are still significantly larger than the as-grown material due to the beneficial effects of the RTA.

Baird *et al.* observed significant In migration into 120 Å wells for furnace-annealed GaInAs/AlInAs quantum wells.[13] The migration of In into the wells was attributed to a chemical potential gradient established by the disparity in the Al and Ga mobilities. (For Si-induced intermixed re-

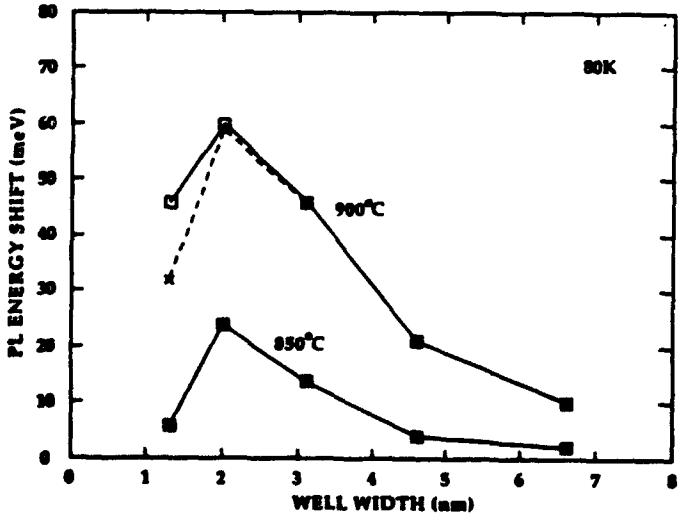

FIG. 2. 80 K PL energy shifts as a function of well width for SiO_2-capped regions relative to as-grown samples (solid lines) or relative to bare regions of the same annealed sample (dashed lines).

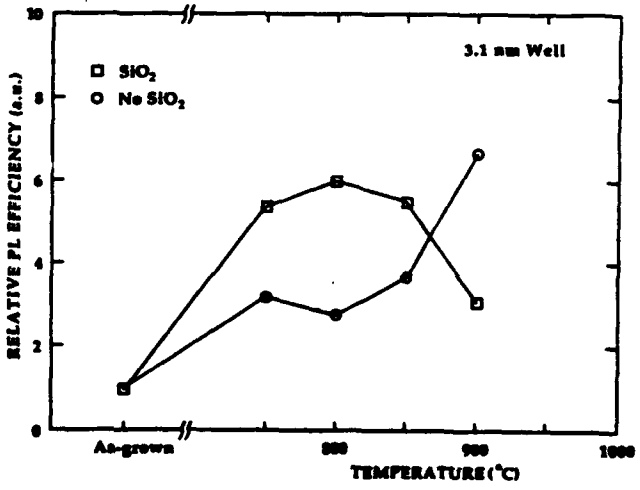

FIG. 3. PL efficiencies (normalized to as-grown samples) for the 3.1 nm well from the SiO_2-capped and bare regions as a function of annealing temperature.

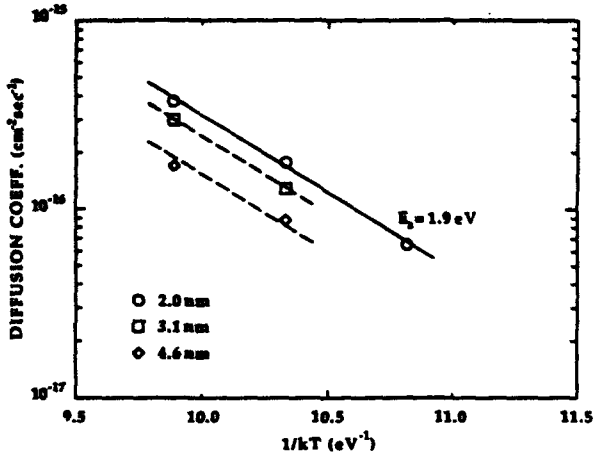

FIG. 4. Arrhenius plots of the diffusion coefficients used to fit the interdiffusion of three of the single quantum wells for the SiO_2-capped regions.

gions, In did not migrate into the wells since the Al and Ga mobilities have equilibrated.) Quantum well calculations estimating the effects of In migration into the wells (which cause well shape changes and strain) always produced decreased transition energies and hence are not consistent with the observed shifting. The migration of In out of the wells could produce positive PL shifts yet would contradict the results of Baird *et al.* and hence suggests that Al-Ga interdiffusion is the primary cause for the shifting.

Assuming that the energy shifts are due to isotropic Al-Ga diffusion at the well/barrier interface, then the interdiffusion coefficient D can be estimated by assuming a complementary error function dependence for the Al composition x, and solve for the subband energies needed to obtain the observed PL shift.[3] Such a model is only an approximation but does account for the two major effects of Al-Ga diffusion: changes in the barrier shape due to Al-Ga diffusion and increased Al in the well itself. Such calculations were completed assuming a 70/30 splitting of the energy-gap discontinuity for the conduction and valence bands, respectively.[3,7,14] The variation of the 300 K band gap was taken to be[15]

$$E_g = 0.76 + 1.04x + 0.87x^2 \text{ (eV)}.$$

Average effective electron masses between 0.06 and $0.07m_0$ were chosen for each well width which gave calculated transition energies within a few meV of the measured as-grown PL peak positions. The use of different masses primarily corresponds to corrections for nonparabolicity.[14] A constant heavy hole effective mass of $0.48m_0$ was used. Figure 4 shows the resulting values of D vs $1/kT$ and yields an activation energy of 1.9 eV. The data form a pattern of roughly parallel lines corresponding to different well sizes. (The dashed lines were constructed by taking lines parallel to the 20 Å well data in order to aid the eye.) Such a pattern of parallel lines could be due to the fact that the calculation does not account exactly for nonparabolicity. A depth dependence to the diffusion process is expected and could also account for a portion of the spread in the diffusion coefficients for the different wells. Seo *et al.* reported an activation energy of 2.3 eV for wells annealed in a RTA environment (with no dielectric cap) which were protected by GaAs proximity caps.[12] It should be noted that the bare regions in our samples showed minimal shifting yet this still suggests that perhaps a similar diffusion mechanism may be involved and would imply that a dominant defect type is shared.

In summary, spatially selective blue shifting up to 74 meV has been observed for GaInAs/AlInAs quantum well transitions due to the presence of a SiO_2 capping layer and is attributed to Al-Ga diffusion. Uncapped regions were left unshifted with much improved PL efficiencies demonstrating that such a process could prove useful in a variety of optical and electrical device applications.

This work was supported in part by the David Sarnoff Research Center, IBM, the Joint Services Electronics Program (F49620-87-C-0044) and Innovative Science and Technology contract No. N00014-86-0521.

[1]R. K. Willardson and A. C. Beer, *Semiconductors and Semimetals*, Vol. 24 (Academic, San Diego, 1987).
[2]H. Z. Chen, A. Ghaffari, H. Morkoç, and A. Yariv, Appl. Phys. Lett. 51, 2094 (1987).
[3]J. D. Ralston, S. O'Brien, G. W. Wicks, and L. F. Eastman, Appl. Phys. Lett. 52, 1511 (1988).
[4]J. D. Ralston, W. J. Schaff, D. P. Bour, and L. F. Eastman, Appl. Phys. Lett. 54, 534 (1989).
[5]L. J. Guido, N. Holonyak, Jr., K. C. Hsieh, R. W. Kaliski, W. E. Plano, R. D. Burnam, R. L. Thorton, J. E. Epler, and T. L. Paoli, J. Appl. Phys. 61, 1372 (1987).
[6]J. Y. Chi, E. S. Koteles, and R. P. Holmstrom, Appl. Phys. Lett. 53, 2185 (1988).
[7]S. O'Brien, D. P. Bour, and J. R. Shealy, Appl. Phys. Lett. 53, 1859 (1988).
[8]Experiments on GaInAs/(Al)GaAs structures also produced large blue shifts only for SiO_2-capped regions.
[9]D. G. Deppe and N. Holonyak, Jr., J. Appl. Phys. 64, R93 (1988).
[10]T. Miyazawa, Y. Suzuki, Y. Kawamura, H. Asai, and O. Mikami, Jpn. J. Appl. Phys. 28, L730 (1989).
[11]L. J. Guido, J. S. Major, Jr., J. E. Baker, and N. Holonyak, Jr., Appl. Phys. Lett. 54, 1265 (1989).
[12]K. S. Seo, P. K. Bhattacharya, G. P. Kothiyal, and S. Hong, Appl. Phys. Lett. 49, 966 (1986).
[13]R. J. Baird, T. J. Potter, R. Lai, G. P. Kothiyal, and P. K. Bhattacharya, Appl. Phys. Lett. 53, 2302 (1988).
[14]D. F. Welch, G. W. Wicks, and L. F. Eastman, J. Appl. Phys. 55, 3176 (1984).
[15]D. Olego, T. Y. Chang, E. Silbert, E. A. Caridi, and A. Pinczuk, Appl. Phys. Lett. 41, 476 (1982).

Selective interdiffusion of GaInAs/AlInAs quantum wells by SiO_2 encapsulation and rapid thermal annealing

S. O'Brien and J. R. Shealy
School of Electrical Engineering, Phillips Hall, Cornell University, Ithaca, New York 14853
V. K. F. Chia
Charles Evans and Associates, 301 Chesapeake Drive, Redwood City, California 94063
J. Y. Chi
GTE Laboratories, Inc., 40 Sylvan Road, Waltham, Massachusetts 02254

(Received 9 July 1990; accepted for publication 25 July 1990)

Substantial blue shifts in the photoluminescence (PL) transition energies of GaInAs/AlInAs single quantum wells were observed due to localized SiO_2 capping and rapid thermal annealing at temperatures between 750 and 900 °C. Secondary-ion mass spectroscopy analyses show that the blue shifts are caused by the impurity-induced interdiffusion of the quantum well interfaces due to the simultaneous diffusion of silicon and oxygen into the crystal. The selective intermixing occurred in regions capped with SiO_2 and exhibited blue shifts up to 74 meV while regions with no SiO_2 showed only minimal shifting. With this band gap change, a lateral index change of approximately 0.6% is anticipated, making this process suitable for index-guided structures. Samples also exhibited up to 26-fold increases in PL efficiencies due to the annealing process. The dependence of energy shifts and PL efficiencies are studied by measuring room-temperature and low-temperature ($\approx$80 K) photoluminescence. Interdiffusion coefficients have also been calculated as a function of temperature.

I. INTRODUCTION

The effects of dielectric encapsulation as a means to effectively control strain, surface stoichiometry, and impurity diffusion profiles in GaAs have been studied and have been used to fabricate novel electrical and optical devices.[1-4] In addition, dielectric encapsulation can also be used to cause enhanced or suppressed diffusion of the group-III or group-V species.[2,5] For example, Guido *et al.* have studied the effects of dielectric encapsulation on furnace-annealed GaAs/AlGaAs quantum well structures and have shown that intermixing, or interdiffusion, of quantum wells can occur for SiO_2 capped structures while for Si_3N_4 capped structures intermixing is suppressed.[6] For the GaAs/AlGaAs material system SiO_2 encapsulation can cause impurity-induced interdiffusion (Si) or impurity-free interdiffusion due to the creation of Ga vacancies in the crystal.[6-8] Similar results have also been observed for strained GaInAs/(Al)GaAs quantum wells.[9] The interdiffusion of quantum well structures is accompanied with effective band gap and refractive index changes which enables the fabrication of numerous unique optical devices (index-guided lasers, transparent waveguides, and multiple wavelength detectors or modulators).[7,10-12] In addition to the numerous device applications, the study of the interdiffusion of GaAs/AlGaAs quantum wells also provides valuable numerical data such as diffusivities, activation energies, and native vacancy concentrations.[8,13,14]

We have extended these studies to the GaInAs/AlInAs material system and have studied the effects of SiO_2 encapsulation and rapid thermal annealing on GaInAs/AlInAs single and multiple quantum wells. $Ga_xIn_{1-x}As/Al_yIn_{1-y}As$ quantum well structures are lattice matched to InP for $x\approx0.47$ and $y\approx0.48$ and exhibit effective band gaps between approximately 1.0 and 1.5 μm (0.83–1.24 eV). Many electro-optical device applications coincide with optical communication systems and require devices to operate in this spectral range. GaInAs/AlInAs quantum well structures have been used to fabricate light-emitting diodes and injection lasers.[15,16] Many of the material transport properties of GaInAs (such as high mobility, low effective mass, high electron velocities, and large Γ-L valley separation) are also very beneficial for ultrafast transistor applications.[17,18]

In this work we show that significant blue-shifting of the PL transition energies occurs for SiO_2 capped GaInAs/AlInAs quantum wells while bare regions are left relatively unaffected. This shifting is shown to be due to impurity-induced disordering due to the fast diffusion of Si and O into the crystal. The disordering process exhibits Al-Ga interdiffusion coefficients of approximately 3×10^{-16} cm^2 s^{-1} at 900 °C and an activation energy of 1.9 eV. In addition we show that the annealing process dramatically improves the photoluminescence efficiencies from the quantum wells which could be very beneficial for optical devices.

II. EXPERIMENTAL PROCEDURE

The GaInAs/AlInAs material used in this work was grown lattice matched on an InP substrate by molecular-beam epitaxy (MBE) and contained a 10-period multiple-quantum well buffer comprised of 1.3 nm wells and 30 nm barriers followed by four single quantum wells with nominal well widths of 6.6, 4.6, 3.1, and 2.0 nm with the thinner wells closer to the surface. The growth finished with a 0.3 μm AlInAs cap. None of the layers were intentionally doped. The 514.5 nm line of an argon-ion laser together with a liq-

 0021-8979/90/225256-06$03.00

uid-nitrogen-cooled Ge detector were used to collect room-temperature and low-temperature photoluminescence (PL) data. Secondary-ion mass spectroscopy (SIMS) data was obtained using a Cameca-IMS-4f ion microanalyzer. Si concentrations were calculated using relative sensitivity factors obtained from the analysis of standard ion implants in AlGaAs. Preliminary analysis of Si revealed ^{28}Si to have negligible interference from $^{27}Al^{1}H$. Therefore, ^{28}Si was used to monitor Si in the samples. Depth scales were obtained by measurements of the analytical craters using an Alpha-Step stylus profilometer and were in basic agreement with the designed growth structure.

The sample preparation included normal surface cleaning with solvents in ultrasonic baths. The SiO_2 was electron-beam evaporated onto shadow-masked samples at pressures of approximately 1×10^{-6} Torr and were post-baked at 150 °C for 1 h. Ellipsometry measurements gave values between 1.45 and 1.49 for the index of refraction of the SiO_2. The samples were cleaved to give pieces containing a few square millimeters of regions with and without SiO_2. All samples were rapid thermally annealed in an argon ambient in an AG Associates Heatpulse 410 rapid thermal annealer using semi-insulating GaAs substrates as proximity caps which provide some protection from As and In desorption for the bare regions. The samples were annealed for 15 s at temperatures between 750 and 900 °C.

III. EXPERIMENTAL RESULTS

The PL linewidths at 5 K, as measured by the full width at half maximum, for the single quantum wells from an as-grown sample varied between 10 and 20 meV while the linewidth from the 1.3 nm multi-quantum wells was 31 meV. When plotted versus well width these values are approximately a factor of 2 below theoretical linewidths calculated on the basis of interface roughness by Singh *et al.* and are comparable to the linewidths measured by Brown *et al.*[19,20] These linewidths indicate that the wells are of fairly good quality. It should be noted that the measured linewidths for all of the wells at 5 K are approximately a constant 6 meV larger then the highest-quality GaInAs/AlInAs quantum wells grown by MBE using ultrahigh-purity Al and In sources.[21] The AlInAs cap layer displayed a linewidth of 19 meV.

PL spectra taken at approximately 80 K from SiO_2 capped and bare regions are presented in Fig. 1. Shown are spectra taken from the SiO_2 capped regions of samples annealed at 850 and 900 °C along with the spectrum from the bare region of a sample annealed at 750 °C. The peak positions for the bare sample annealed at 750 °C and the as-grown material are identical. Significant blue-shifting is clearly evident for the SiO_2 capped regions and is indicative of intermixed quantum wells. As an example, the 2.0 nm well exhibited a blue shift of approximately 60 meV for the 900 °C anneal. The magnitude of the blue-shifting, as measured by the PL ($\approx$80 K), for the 3.1 nm well are shown in Fig. 2 for the bare and SiO_2 capped regions as a function of annealing temperature (solid lines and symbols). The bare regions show almost no blue-shifting (only 3 meV for the 900 °C anneal) while the SiO_2 capped regions showed continuous

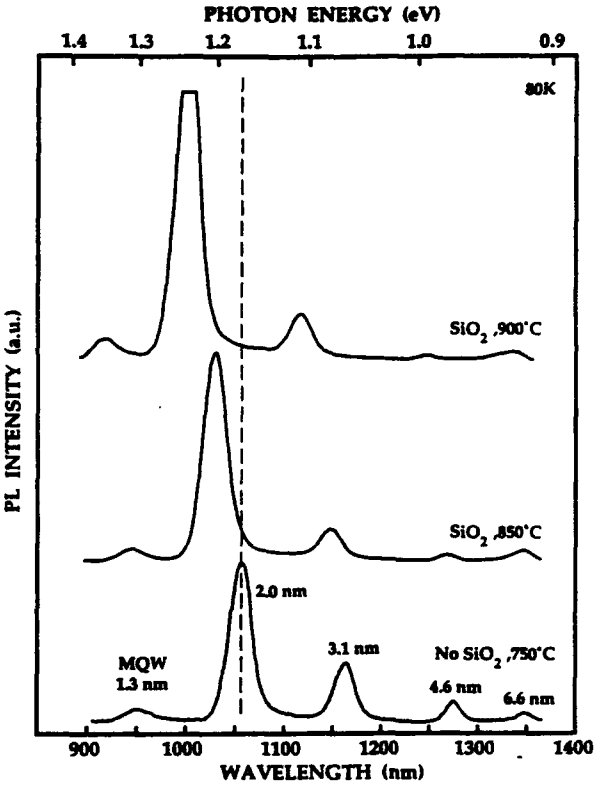

FIG. 1. Low-temperature PL ($\approx$80 K) spectra from the AlInAs/GaInAs samples containing a multiple quantum well buffer and four single quantum wells annealed at various temperatures with or without SiO_2 capping.

shifting up to 46 meV. The ratio of the blue-shifting for the SiO_2 capped region to the bare region grows to 16:1 for the 900 °C anneal, which shows a high selectivity for the intermixing process.

The PL efficiencies from the wells are also significantly affected by the intermixing. The PL efficiencies for the 3.1 nm well are also shown in Fig. 2 for the SiO_2 capped and bare regions of the samples as a function of annealing temperature (open symbols and dashed lines). The PL efficiencies are measured relative to the same well on an as-grown sam-

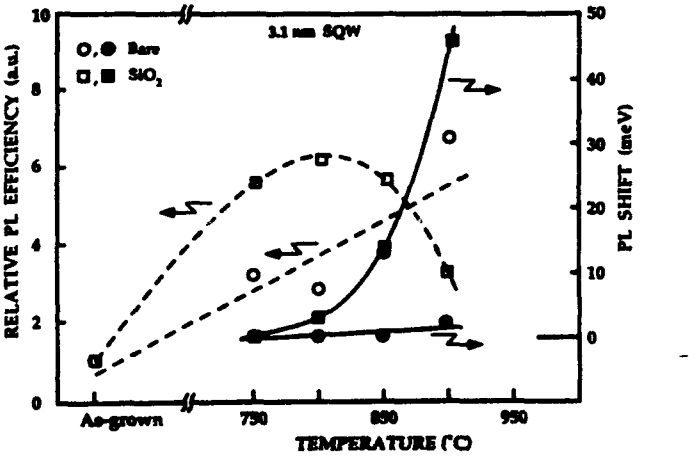

FIG. 2. PL efficiencies (dashed lines) and the magnitude of blue-shifting (solid lines) for the 3.1 nm well as a function of annealing temperature. Data are shown for the bare (circles) and SiO_2 capped regions (squares).

ple. The bare regions show a roughly linear increase in efficiency where for the 900 °C anneal the efficiency has increased by almost a factor of 7. The SiO_2 capped regions initially exhibit the same increasing trend yet for the higher temperatures the PL efficiencies deviate from this pattern by showing substantial decreases. It is for these temperatures that the wells show significant blue-shifting and are partially intermixed. However, it should be noted that the partially intermixed wells exhibit efficiencies which are still significantly larger than those from the as-grown wells. The same trends were also observed for the other wells. The intermixed wells (SiO_2 capped) also exhibited linewidths which were approximately 10% larger than the annealed and unintermixed wells.

The improvements in the PL efficiencies from the bare regions also showed a strong dependence with well width and data for the different annealing temperatures are shown in Fig. 3. From this plot it is clear that the PL efficiency improves dramatically for each well as the annealing temperature is increased. For the 6.6 nm well the increase is approximately 26-fold. In addition, for each annealing temperature the PL efficiencies also improved more for the larger wells producing approximately linear curves. This was most dramatic for the 850 and 900 °C anneals. One possible explanation of this trend is that nonradiative defects are annealed out of the GaInAs well material except near the interfaces.[22,23] Hence, the larger wells exhibit large improvements in PL efficiency yet for the smaller wells the nonradiative defects in the vicinity of the interfaces still occupy a significant portion of the well. The linewidths of the PL transitions from the bare and annealed regions remained the same as those measured for the as-grown wells.

Room-temperature PL measurements were also taken and spectra from a sample annealed at 900 °C for 15 s is shown in Fig. 4. The blue shifting of the PL from the SiO_2 capped region is clearly evident although the magnitude of the shifting at 300 K was always consistently larger than the shifting measured at 80 K. For example, the blue shifting at 300 K for the 2.0 and 3.1 nm wells at all of the various annealing temperatures were approximately 14 ($\pm$ 3) and 6

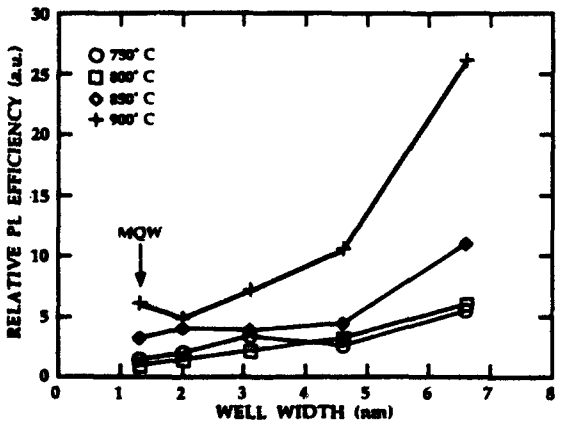

FIG. 3. PL efficiencies (normalized to the same well on an as-grown sample) from the bare regions for different annealing temperatures as a function of well width.

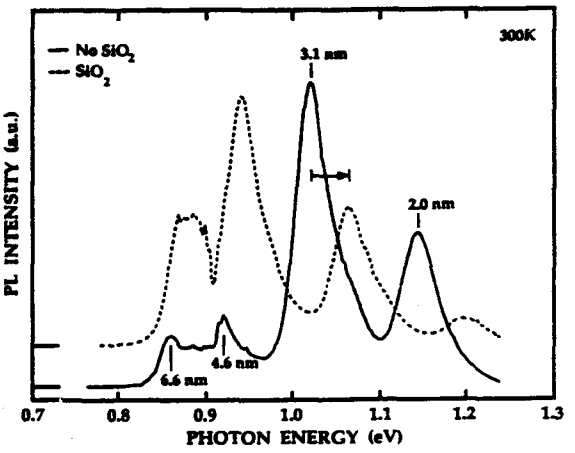

FIG. 4. Room-temperature PL spectra from the SiO_2 capped and bare regions of a sample annealed at 900 °C for 15 s.

($\pm$ 2) meV larger, respectively. The specific reason for these differences have not been studied in detail yet different well shapes due to temperature and strain effects could possibly account for this behavior. (Simple quantum well calculations showed that up to 5 meV of these differences in energy shifts could be due to having slightly different well depths for each measurement temperature. This small temperature dependence is due to nonlinear band gap relationships and the effects of different thermal expansion coefficients for the well and barrier materials. The existence of strained alloy material near the interfaces of the intermixed well could also cause small changes in the well shape.) Using a linear extrapolation between the band gap and the index of refraction, the magnitude of the observed band gap shifts at room temperature ($\approx$74 meV) would correspond to a change in refractive index of approximately 0.6%, making the intermixing process suitable for index-guided structures. The blue shifts measured at 300 K are used later to calculate the Al-Ga interdiffusion coefficients as a function of annealing temperature.

To investigate the cause of the interdiffusion, SIMS was used to investigate the compositional profiles of the annealed samples. Several analyses were performed on each sample to confirm reproducibility. SIMS data taken from the bare and SiO_2 capped regions of a sample annealed at 900 °C for 15 s are shown in Figs. 5(a) and 5(b), respectively. The Al and In profiles for the uncapped sample clearly delineates the epitaxial structure of the samples. The four single quantum wells along with the 10-period superlattice buffer are clearly visible in the Al profile. For the SiO_2 capped region, significant diffusion of Al is apparent as evidenced by a definite slope in the Al profile, smaller signals from the wells, and significant changes in the epitaxial interface at a depth of approximately 0.7 μm. The In profiles from both regions were almost identical showing that enhanced In diffusion was not evident. A large amount of Si diffusion into the capped structure is apparent. Approximately 3–4 orders of magnitude more Si appears in the capped region. The Si signal drops by approximately two orders of magnitude at a depth of 1 μm, yielding an estimate for the diffusion coefficient for the Si of approximately 7×10^{-10} cm^2 s^{-1}. This

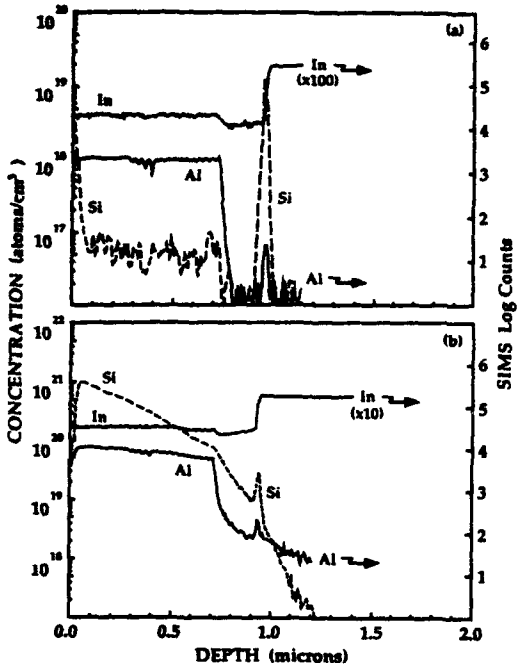

FIG. 5. SIMS depth profiles for In, Al, and Si from the bare (a) and SiO_2 capped (b) regions of a sample annealed at 900 °C for 15 s.

value is comparable to the large diffusion coefficients observed for Zn in GaAs.[24] This diffusion of Si into the crystal is very similar to that observed for SiO_2 capped and furnace-annealed AlGaAs structures and was attributed to the reduction of the SiO_2 to form free Si and O.[7] Compensation of the Si was also observed by Guido *et al.* due to the additional diffusion of oxygen into the crystal which yielded higher resistivity intermixed crystal. Significant oxygen incorporation into the GaInAs/AlInAs quantum well material was also observed using SIMS. The depth profiles for oxygen from the bare (no SiO_2) and the SiO_2 capped regions are shown in Fig. 6. There is approximately 2–3 orders of magnitude more oxygen in the SiO_2 capped sample. Miyazawa *et al.* observed significant broadening of the PL transitions due to increased background doping for Si impurity-induced disordered GaInAs/AlInAs quantum wells.[25] The linewidths of the PL transitions from the SiO_2 capped and intermixed wells in this work showed only 10% increases which would indicate that the O is compensating the Si. Also shown in Fig. 6 is the Si profile from the SiO_2 capped region of the same sample. To within experimental error, the Si profile almost exactly matches the O profile implying that the Si and O diffuse together. This may suggest that the Si and O are diffusing as donor-acceptor pairs which is analogous to a Si-Si pair diffusion model for GaAs proposed by Greiner and Gibbons.[26]

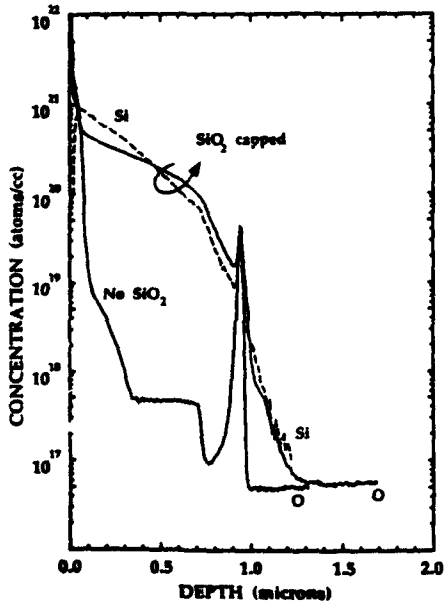

FIG. 6. SIMS depth profiles for oxygen from the bare and SiO_2 capped regions of a sample annealed at 900 °C for 15 s (solid lines). Also shown is the Si profile from the SiO_2 capped and annealed region (dashed line).

Impurity-induced interdiffusion has been observed by Baird *et al.* for Si-implanted and annealed GaInAs/AlInAs quantum well structures where Si concentrations were higher than a threshold value of approximately 1.5×10^{19} cm^{-3}.[27] A similar phenomena is occurring here except the Si source is from the SiO_2 cap and O is also diffusing into the crystal. Assuming that the PL energy shifts are due to isotropic Al and Ga diffusion then estimates for the Al-Ga interdiffusion coefficients can be obtained through the following error function dependence for the Al composition for a well centered at $z = 0$ (Refs. 8 and 28):

$$x(z) = x_0\left[1 + \frac{1}{2}\,\mathrm{erf}\left(\frac{z - L_z/2}{2\sqrt{Dt}}\right) - \frac{1}{2}\,\mathrm{erf}\left(\frac{z + L_z/2}{2\sqrt{Dt}}\right)\right]. \tag{1}$$

In this equation x_0 is the initial Al composition of the barrier, L_z is the well width, D is the Al-Ga interdiffusion coefficient, t is the annealing time, and $\mathrm{erf}(y)$ is the error function. An example of the shape of the conduction band for an interdiffused 4.6 nm well ($D = 2\times10^{-16}$ cm^2 s^{-1}) along with the first bound state energies are shown as an inset in Fig. 7. The $n = 1$ bound states for the electron and hole wells im-

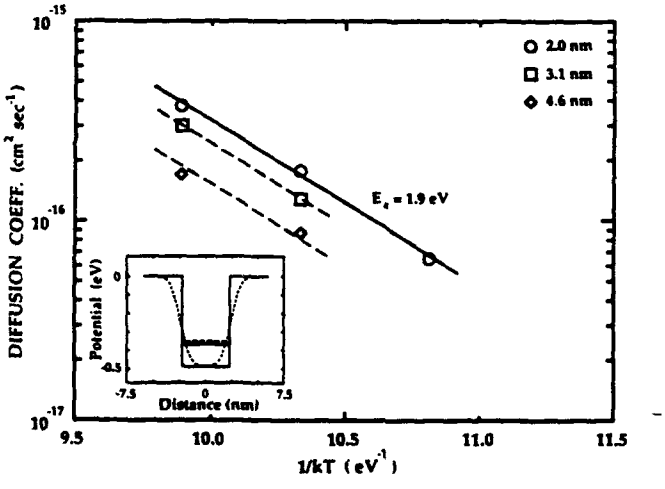

FIG. 7. Arrhenius plot of the diffusion coefficients used to fit the interdiffusion of three of the single quantum wells of the SiO_2 capped and annealed samples. Shown as an inset is an example of the electron potential well profile for the as-grown 4.6 nm square well and a partially intermixed well with $D = 2\times10^{-16}$ cm^2 s^{-1}.

plied by Eq. (1) are obtained by integrating the Schrödinger equation numerically assuming a 70/30 splitting of the energy gap discontinuity for the conduction and valence bands, respectively.[29] The variation of the 300 K band gap of $Al_xGa_{0.47-x}In_{0.53}As$ was taken to be[30]

$$E_g = 0.76 + 1.04x + 0.87x^2 \text{ (eV)}$$

Average effective electron masses between 0.06 and $0.07m_0$ were chosen for each well width which gave calculated transition energies within a few meV of the measured as-grown PL peak positions.[31] The use of different masses primarily correspond to corrections for nonparabolicity.[29] A constant heavy-hole effective mass of $0.48m_0$ was used. For each annealing temperature the diffusion coefficient is varied until a value is obtained which gives the experimentally observed blue-shifted PL peak position. The resulting diffusion coefficients are plotted versus $1/kT$ in Fig. 7 for the 2.0, 3.1, and 4.6 nm wells and exhibit an activation energy of approximately 1.9 eV. The data form a pattern of roughly parallel lines corresponding to the different well sizes. (The dashed lines were constructed by taking lines parallel to the 2.0 nm well data in order to aid the eye.) Such a pattern of parallel lines could easily be due to the fact that the calculation does not account exactly for nonparabolicity. This activation energy is approximately a factor of 2 smaller than that observed for GaAs/AlAs superlattices.[8,32] In a study of the thermal stability of GaInAs/AlInAs quantum wells Seo *et al.* reported an activation energy of 2.3 eV for wells annealed in a RTA environment (with no dielectric cap) which were protected by GaAs proximity caps.[33] In addition, the interdiffusion coefficients determined by Seo *et al.* were about an order of magnitude larger than those for the SiO_2 capped and impurity-induced intermixed regions studied in this work. This implies that the diffusion coefficients for the respective bare regions would differ by at least two orders of magnitude. (The bare regions in this work showed absolutely minimal shifting.) This suggests that the interdiffusion of the wells used by Seo *et al.* was dominated by an intrinsic defect and are not indicative of the thermal stability of undoped GaInAs/AlInAs quantum wells. Furthermore, the similar activation energies suggests that the interdiffusion mechanism may also be similar.

IV. DISCUSSION AND SUMMARY

Two other works have reported on the Si impurity-induced disordering of GaInAs/AlInAs quantum wells.[25,27] In one case the Si was incorporated into the crystal during growth while for the other case a Si implantation process was used. The incorporation of Si during crystal growth is not useful for device structures since it may severely degrade the optical quality of the crystal. In this work, SIMS analyses showed that impurity-induced intermixing occurred due to the extremely fast diffusion of Si and O into the crystal and is caused by the SiO_2 cap being in contact with AlInAs. It is important to note that the SiO_2 capping process is very easy to perform and is much less expensive than ion implantation. In addition, the simultaneous incorporation of O into the crystal is likely compensating the Si leaving higher-resistivity interdiffused crystal which could be advantageous for a number of optical device structures.

Two other works have also reported on impurity-free intermixing processes for GaInAs/AlInAs structures.[34,35] Chi *et al.* observed impurity-free intermixing for the bare regions of samples while SiO_2 capped regions were left unaltered. The effects of arsenic overpressure on the formation of point defects which promote the diffusion of the III-V atomic species can be dramatic and can easily explain these results since GaAs proximity caps were not used.[36] Miyazawa *et al.* have shown that partial intermixing occurs for Si_3N_4 capped GaInAs/AlInAs multi-quantum wells which are only *repetitively* rapid thermally annealed. Both SiO_2 and Si_3N_4 have been used to intermix GaAs/AlGaAs and GaInAs/(Al)GaAs structures in an impurity-free manner.[2,8,9] It is very likely that strain at the semiconductor/dielectric interface due to the annealing process is serving as a catalyst for Ga to diffuse out of the crystal and into the porous dielectric leaving a significant number of Ga vacancies which provide enhanced group-III diffusion.[2,37,38] As extensive studies with GaAs/AlGaAs have shown, the condition of the crystal near the surface (Al content or doping levels) and the characteristics of the capping material (strain, porosity, or As overpressure) are very critical for determining the intermixing mechanism for GaAlInAs quantum wells as well.[6,36]

The rapid thermal annealing in this work also significantly improved the PL efficiencies from the quantum wells where for the largest well an improvement of over 26-fold was measured. The improvement in the PL efficiencies from the bare and annealed regions showed a clear trend with well width, suggesting that the efficiencies from the smaller wells are dominated by nonradiative defects "pinned" near the interfaces. Historically, injection lasers in this material system have required very large currents for operation, however, with these large improvements in the PL efficiency the fabrication of higher-quality lasers, and other optical devices, may be possible.

ACKNOWLEDGMENTS

The authors would like to express their thanks to L. Elbaum and D. P. Bour for acquiring some of the PL data. This work was supported in part by the David Sarnoff Research Center, the Joint Services Electronics Program (F49620-87-C-0044), Innovative Science and Technology contract No. N00014-86-0521 and IBM.

[1] P. A. Kirby, P. R. Selway, and L. D. Westbrook, J. Appl. Phys. 50, 4567 (1979).
[2] J. Gyulai, J. W. Mayer, I. V. Mitchell, and V. Rodriguez, Appl. Phys. Lett. 17, 332 (1970).
[3] C. Blaauw, A. J. Springthorpe, S. Dzioba, and B. Emmerstorfer, J. Electron. Mater. 13, 251 (1984).
[4] W. X. Zou, G. A. Vawter, J. L. Merz, and L. A. Coldren, J. Appl. Phys. 62, 828 (1987).
[5] I. Ohdomari, S. Mizutani, H. Kume, M. Mori, I. Kimura, and K. Yoneda, Appl. Phys. Lett. 32, 218 (1978).
[6] L. J. Guido, N. Holonyak, Jr., K. C. Hsieh, R. W. Kaliski, W. E. Plano, R. D. Burnam, R. L. Thorton, J. E. Epler, and T. L. Paoli, J. Appl. Phys. 61, 1372 (1987).
[7] L. J. Guido, J. S. Major, Jr., J. E. Baker, and N. Holonyak, Jr., and R. D. Burnham, Appl. Phys. Lett. 54, 1265 (1989).

[9] J. D. Ralston, S. O'Brien, G. W. Wicks, and L. F. Eastman, Appl. Phys. Lett. 52, 1511 (1988).
[9] S. O'Brien, Ph. D. thesis, Cornell University, 1990.
[10] R. L. Thornton, W. J. Mosby, and H. F. Chung, Appl. Phys. Lett. 53, 2669 (1988).
[11] J. Werner, E. Kapon, A. C. VonLehmen, R. Bhat, E. Colas, N. G. Stofel, and S. A. Schwarz, Appl. Phys. Lett. 53, 1693 (1988).
[12] B. C. Johnson, J. C. Campbell, B. D. Dupuis, and B. Tell, Electron. Lett. 24, 181 (1988).
[13] K. B. Kahen, G. Rajeswaran, and S. T. Lee, Appl. Phys. Lett. 53, 1635 (1988).
[14] L. J. Guido, N. Holonyak, Jr., and K. C. Hsieh, Inst. Phys. Conf. Ser. 96, 353 (1988).
[15] D. F. Welch, G. W. Wicks, D. W. Woodard, and L. F. Eastman, J. Vac. Sci. Technol. B 1, 202 (1983).
[16] H. Temkin, K. Alavi, W. R. Wagner, T. P. Pearsal, and A. Y. Cho, Appl. Phys. Lett. 42, 845 (1983).
[17] U. K. Mishra, A. S. Brown, L. M. Jelloian, M. Thompson, L. D. Nguyen, and S. E. Rosenbaum, IEDM Tech. Dig., 101 (1989).
[18] J. L. Kuang, P. J. Tasker, Y. K. Chen, G. W. Wang, L. F. Eastman, O. A. Aina, H. Hiem, and A. Fathimulla, Appl. Phys. Lett. 54, 1136 (1989).
[19] A. S. Brown, J. A. Henige, and M. J. Delaney, Appl. Phys. Lett. 52, 1142 (1988).
[20] J. Singh and K. K. Bajaj, J. Appl. Phys. 57, 5433 (1985).
[21] T. Mishima, J. Kasai, Y. Uchida, and S. Takahashi, J. Cryst.Growth 95, 338 (1989).
[22] K. Jagannadham and J. Narayan, Mater. Res. Soc. Symp. Proc. 91, 365 (1987).
[23] J. M. Phillips, J. L. Batstone, and L. Pfeiffer, Mater. Res. Soc. Symp. Proc. 91, 81 (1987).
[24] H. C. Casey, Jr., M. B. Panish, and L. L. Chang, Phys. Rev. 162, 660 (1967).
[25] T. Miyazawa, Y. Kawamura, and O. Mikami, Jpn. J. Appl. Phys. 27, L1371 (1988).
[26] M. E. Greiner and J. F. Gibbons, J. Appl. Phys. 57, 5181 (1986).
[27] R. J. Baird, T. J. Potter, R. Lai, G. P. Kothiyal, and P. K. Bhattacharya, Appl. Phys. Lett. 53, 2302 (1988).
[28] T. E. Schlesinger and T. Kuech, Appl. Phys. Lett. 49, 519 (1986).
[29] D. F. Welch, G. W. Wicks, and L. F. Eastman, J. Appl. Phys. 55, 3176 (1984).
[30] D. Olego, T. Y. Chang, E. Silbert, E. A. Caridi, and A. Pinczuk, Appl. Phys. Lett. 41, 476 (1982)
[31] K. -H. Hellwege, *Landolt-Bornstein: Numerical Data and Functional Relationships in Science and Technology*, Vol. 17 (Springer, Berlin, 1982).
[32] P. Mei, H. W. Yoon, T. Venkatesan, S. A. Schwartz, and J. P. Harbison, Appl. Phys. Lett. 50, 1823 (1987).
[33] K. S. Seo, P. K. Bhattacharya, G. P. Kothiyal, and S. Hong, Appl. Phys. Lett. 49, 966 (1986).
[34] J. Y. Chi, E. S. Koteles, and R. P. Holmstrom, Appl. Phys. Lett. 53, 2185 (1988).
[35] T. Miyazawa, Y. Suzuki, Y. Kawamura, H. Asai, and O. Mikami, Jpn. J. Appl. Phys. 28, L730 (1989).
[36] D. G. Deppe and N. Holonyak, Jr., J. Appl. Phys. 64, R93 (1988).
[37] M. Katayama, Y. Tokuda, N. Ando, and Y. Inoue, Appl. Phys. Lett. 54, 2559 (1989).
[38] S. Mizutani, I. Ohdomari, T. Miyazawa, T. Iwamori, I. Kimura, and K. Yoneda, Appl. Phys. Lett. 53, 1470 (1982).